



Published in final edited form as:

Dig Liver Dis. 2017 February ; 49(2): 188–196. doi:10.1016/j.dld.2016.11.008.

CD98 siRNA-loaded nanoparticles decrease hepatic steatosis in mice

Brandon S.B. Canup¹, Heliang Song¹, Vu Le Ngo², Xiangxiao Meng¹, Timothy L. Denning², Pallavi Garg², and Hamed Laroui^{1,2}

¹Department of Chemistry, Center for Diagnostics and Therapeutics, Georgia State University, Atlanta, GA, USA.

²Department of Biology, Center for Diagnostics and Therapeutics, Georgia State University, Atlanta, GA, USA.

Abstract

Non-alcoholic fatty liver disease (NAFLD) is characterized by excessive lipid hepatic accumulation. Here, we investigated whether a reduction of CD98 expression mediated by CD98 siRNA-loaded nanoparticles (NPs) could attenuate liver disease markers in a mouse model of NAFLD. NPs were generated using a double emulsion/solvent evaporation technique. Mice fed a high fat diet for 8 weeks to induce fatty liver were treated with vein tail injections of CD98 siRNA-loaded NPs. In vitro, HepG2 treated with CD98 siRNA-loaded NPs showed significant downregulation of CD98 leading to a significant decrease of major pro-inflammatory cytokines and markers. In vivo, CD98 siRNA-loaded NPs strongly decreased all markers of NAFLD, including the blood levels of ALT and lipids accumulation, fibrosis evidence and pro-inflammatory cytokines. In conclusion, our results indicate that CD98 appears to function as a key actor/inducer in NAFLD, and that our NPs approach may offer a new targeted therapeutic for this disease.

Keywords

Hepatic CD98; targeted therapeutic strategy; siRNA-loaded nanoparticles; nonalcoholic fatty liver

Background

Non-alcoholic fatty liver disease (NAFLD) is highly correlated to obesity and insulin resistance. It is a major problem as many studies have strongly correlated NAFLD with non-alcoholic steatohepatitis (NASH) and its possible pathogenesis to more dramatic liver diseases^{1,2}, such as cirrhosis and hepatocellular carcinoma (HCC). Thus, this “benign” liver-associated disease has been increasingly studied in the past decade^{1–3}.

Corresponding author: Dr. Hamed Laroui, Corresponding-Authors, Petit Science Center, 100 Piedmont Ave., PSC522, Atlanta, GA 30303, USA. (Tel: +1 404 413 5754), hlaroui@gsu.edu.

Authors' contributions: Conception and design: HL, TLD; Development of Methodology: HL, PG; Acquisition of data: BSBC, HS, VLN, XM; Analysis and interpretation of data: HL, BSBC, HS, VLN, XM, PG, TLD; Writing, review, and/or revision of manuscript: HL; Study supervision: HL.

Competing interests: No potential conflicts of interest were disclosed by the authors.

The liver contributes to multiple functions, including: carbohydrate metabolism, plasma protein synthesis, digestion, the disposal of drugs, toxins and hormones, phagocytosis, and the metabolism of lipids, proteins and amino acids ⁴. Some of the major diseases of the liver include fatty liver diseases (FLD), NASH, hepatitis B and C, fibrosis, cirrhosis, and HCC. FLD is classified into two types: NAFLD and alcoholic fatty liver disease (AFLD). NAFLD, which is very common in adults and children of Western society due to the common consumption of a high fat diet, is defined as lipid accumulation which progressively leads to NASH and dramatically increases the risks of cirrhosis, liver failure, and HCC ^{5,6}. The pathogenesis of NAFLD is poorly understood, but the disease has been associated with a number of metabolic conditions including: insulin resistance, lipidemia and hepatic fibrosis ^{7,8}. Several theories have been put forth to explain the development of NAFLD. The most prominent is the multi-hit hypothesis, which states that NAFLD begins with insulin resistance, which leads to the oxidization of lipids and the release free fatty acids. In the first hit, the free fatty acids are repacked as triglycerides, which are stored in fat vacuoles in the liver, causing hepatic steatosis ⁷. In the second hit, lipid oxidation causes oxidative damage through the production of reactive oxygen species (ROS) and inflammatory mediators, such as tumor necrosis factor α (TNF- α), IL-6, cyclooxygenase 2 (Cox-2) and interferon gamma (IFN- γ) ⁷. This damage disrupts apoptosis and allows the hepatic steatosis to progress to NASH ⁷.

CD98 is a cell-surface amino-acid transporter formed by covalent linkage of the CD98 heavy chain (CD98hc) with several different light chains (CD98lc). In this study, we targeted CD98 by siRNA strategy to reduce the CD98hc. The justification of our strategy is that CD98hc has particularly the function of a β 1-integrin regulator and can be modulated by IFN- γ ^{9,10}. The glycoprotein-associated transporters are a novel class of amino acid transporters that have gained recent research interest, not only in relation to transport, but regarding the CD98-linked functions in cell activation, integrin signaling, cell fusion and malignant transformation ^{11,12}. In the context of intestinal inflammation, multiples studies have shown that pro-inflammatory cytokines upregulate CD98 expression, and that CD98 is a pro-inflammatory receptor involved in many inflammation-related diseases and cancers of various organs, including the intestinal tract ¹³⁻¹⁶ and lungs ^{17,18}. Thus, blocking the progression of CD98 liver expression at an early stage of the disease inflammation could represent a key therapeutic strategy for attenuating the transition of NAFLD to cirrhosis or HCC.

CD98 has not been extensively studied in the liver, except in the context of HCC ¹⁹. The significance of our study is to show that modulation of hepatic CD98 expression could represent a promising therapeutic strategy for treating and preventing hepatic diseases, such as NAFLD. To test this hypothesis, we first tested CD98 siRNA-loaded NPs on HepG2 cells and generated a mouse model of liver inflammation using a high-fat diet. Then, we treated the mice with CD98 siRNA-loaded NPs to decrease the liver CD98 expression.

Methods

Analysis of human samples biopsies stained for CD98

See Supplementary Materials and Methods

Preparation of CD98 siRNA/PEI-loaded NPs covered with PVA

NPs were synthesized via double emulsion/solvent evaporation, as described previously²⁰. An internal phase (see details below) containing the drug was mixed with 20 g/L of polylactic acid (PLA) in dichloromethane to generate a water-in-oil (W/O) emulsion after 2 min of vortexing (Maxi Mix II, Thermodyne, Dubuque, Iowa) and 1 min of sonication with 50% active cycles at 70% power ($P_{\max}=400$ W) (Digital Sonifier 450, Branson, Danbury, CT). This first emulsion was dropped in a second water phase containing 0.3g/L of PVA to generate a water/oil/water emulsion (W/O/W).

The W/O/W emulsion was dropped in a dispersing phase of 0.1g/L polyvinyl alcohol (PVA), and stirred at 45°C under a vacuum to remove dichloromethane. NPs were centrifuged at 9953g and freeze-dried overnight at -50°C under 0.1 mbar pressure. As the second emulsion allowed PVA to be grafted on the surface by hydrophobic interaction with the PLA matrix, NPs were coated with PVA to prevent aggregations through electrostatic repulsions.

Preparation of the internal phase

The internal phase has a typical N/P ratio of the number of negative charges of siRNA (CD98 siRNA or FITC-CD98 siRNA or scrambled siRNA) (P as the phosphorous charge) and positive charges of PEI (N as the ammonium charge) (N/P ratios of 30 for PEI/siRNA). A mixture of siRNA/PEI: 29 μ L CD98 siRNA (5 μ M) was combined with 18 μ L PEI (5mM), and incubated for 10 min at room temperature for complexation. After 10 min, a polyplex was formed, and 750 μ L bovine serum albumin (BSA, 50g/L) added, generating the first emulsion with dichloromethane.

SEM

See Supplementary Materials and Methods

AFM Measurement

See Supplementary Materials and Methods

NPs size and zeta potential measurements

See Supplementary Materials and Methods

WST-1

See Supplementary Materials and Methods

Cell Culture and Lipopolysaccharides (LPS) induction

See Supplementary Materials and Methods

Intracellular NP uptake visualization

See Supplementary Materials and Methods

Mice

See Supplementary Materials and Methods

Oil red (or lipid vacuoles) staining and Hematoxylin and Eosin Y and red Sirius Staining Protocol

See Supplementary Materials and Methods

Western Blot of Liver Samples

See Supplementary Materials and Methods

Elisa for secreted cytokines on HepG2 cells

See Supplementary Materials and Methods

Flow Cytometry

See Supplementary Materials and Methods

Results

Hepatic CD98 is overexpressed in human liver biopsies from NAFLD patients

In tissue samples from humans of various ages, genders and liver pathologies, CD98 expression was assessed by immunohistochemistry staining. Supplementary Figure 1 represented two selected and significant examples of CD98 staining on human liver biopsies: a healthy 56-year-old man (Supplementary Figure 1A) and a 58-year-old man with nonalcoholic fatty liver (Supplementary Figure 1B). Compared to the basal expression of CD98 (brown staining obtained by classic immunohistochemistry staining) in the healthy liver tissue sample (Supplementary Figure 1A), the CD98 levels were significantly increased in the NAFLD patient. Pathological analysis of the liver tissues from NAFLD patients also showed major immune cells infiltration (circles on Supplementary Figure 1B). Interestingly, we observed overexpression of CD98 (brown staining) in membrane surfaces of both hepatocytes and immune cells. Based on this extensive observation, we hypothesized that the downregulation of hepatic CD98 could dramatically counter the pro-inflammation caused by NAFLD in the liver. This data demonstrates the potential of CD98, not only as a marker of liver disease severity, but also as a potential therapeutic target for the treatment of liver disease.

Synthesis and characterization of CD98 siRNA-loaded poly(lactic acid) (PLA) NPs

CD98 siRNA-loaded NPs were successfully synthesized using our previously described method^{21–27}. In short, double emulsion/evaporation of organic solvent was used to encapsulate the CD98 siRNA inside PLA matrix-based NPs. To ensure that the siRNAs would be released in the cytosol (a prerequisite for CD98 knockdown), we electrostatically pre-complexed the CD98 siRNA with a short-chain polyethylenimine (PEI). This should disrupt the endosomal membrane according to the principle of the proton-sponge effect and extend the duration over which the siRNA is released^{22,24,27}.

Using scanning electron microscopy, the NPs were estimated at 275 nm in diameter and showed a homogeneous distribution (Figure 1A). This result was confirmed using atomic force microscopy, which showed a homogenous distribution centered on a diameter of 280 nm (Figure 1B).

PEI/siRNA complex insured a “long lasting release profile” of the CD98 siRNA from the NPs (Figure 1C). In Figure 1C, the “burst effect” (early and significant release of a drug from drug-loaded NPs)^{22,24,27} was not seen in our system: 60–70% of the active principle remained inside the NPs after a 4-h incubation in PBS (Figure 1C). This laps of time is relatively large for liver cells to take up the NPs from the blood stream (shown later in the study). Finally, we used dynamic light scattering to further confirm the size of the NPs and assess their surface charge. The diameter was confirmed to be around 275 nm, and the charge of the siRNA-loaded NPs was around -12.84 mV (Figure 1D). This charge was consistent to insure optimal interactions with cell membranes, and the absolute value of the charge was enough to prevent NPs from agglomerating via electrostatic repulsions²⁸. As shown in Figure 1E, we studied the cytotoxicity of the CD98 siRNA-loaded NPs on HepG2 cell monolayers, and found that treatment of cells with 1 mg/mL of the NPs for 72 h did not have any cytotoxic effect in this system (98.56% viable cells). Similar results were obtained in Caco2-BBE and RAW 264.7 cells^{13,29–33}.

CD98 siRNA-loaded NPs were significantly uptaken by HepG2, Caco2-BBE and Raw 264.7 cells, and CD98 knockdown attenuated mRNA expressions of major pro-inflammatory markers

The in vitro uptake of NPs by cells is a critical parameter in testing the efficiency of a potential therapeutic vector. FITC-tagged CD98 siRNA-loaded NPs were significantly uptaken by a monolayer of HepG2 cells (Figure 2A). The bright signal associated with the FITC-tagged siRNA was significantly observed both at the membrane (early stage of endocytosis) and in the cytosol (late stage of endocytosis). Furthermore, the integrity and intracellular efficiency of the CD98 siRNA encapsulated in NPs was demonstrated measuring the expression level of CD98 by quantitative real time polymerase chain reaction (qRT-PCR). The uptake of CD98 siRNA-loaded NPs by cells (Caco2-BBE, RAW 264.7 and HepG2 cells) was also examined after lipopolysaccharide (LPS) stimulation in vitro. LPS stimulation (10 μ g/mL LPS for a period of 24h) was found to increase CD98 mRNA expression level compared to non-stimulated cells measured by qRT-PCR (Figure 2B). Pretreatment of cells with CD98 siRNA-loaded NPs significantly downregulated the LPS-mediated induction of CD98 by 7- (Raw 264.7), 6- (HepG2), and 8- (Caco2-BBE) times compared to cells that were treated with control scrambled siRNA-loaded prior to LPS stimulation. Pretreatment with CD98 siRNA-loaded NPs also decreased the LPS-mediated upregulation of pro-inflammatory markers, including IL1- β (7-fold for Raw 264.7 cells, 6-fold for HepG2 cells, and 10-fold for Caco2-BBE cells; Figure 2C), IFN- γ (10-fold, 6-fold, and 2-fold, respectively; Figure 2D), Cox-2 (5-fold, 4-fold, and 5-fold, respectively; Figure 2E), and TNF- α (90-fold, 10-fold and 10-fold, respectively; Figure 2F).

Collectively, our in vitro experiments showed that the CD98 siRNA-loaded NPs could efficiently downregulate CD98 and key regulators of inflammation. Therefore, we next tested these NPs in the high fat diet-induced mouse model of NAFLD.

CD98 siRNA-loaded NPs significantly reduced the secreted protein expressions of TNF- α , IL-6 and IFN- γ on HepG2 cells stimulated by LPS.

The reduction of major pro-inflammatory player shown by mRNA quantification (Figure 2 B-F) was confirmed by secreted protein quantification of TNF- α , IL-6 and IFN- γ (Supplementary Figure 2). Based on ELISA quantification, Supplementary Figure 2A, B and C showed, respectively, the reduction of secretion of TNF- α by 14% (Supplementary Figure 2A), IL-6 by 6% (Supplementary Figure 2B) and IFN- γ by 500% (Supplementary Figure 2C). Altogether, the results based on cells shown in Figure 2A-F and Supplementary Figure 2A-C demonstrated that CD98 siRNA loaded NPs were effectively uptaken and the siRNA was released inside cells. This cytosolic release led to a reduction of all major pro-inflammatory signals via CD98 knockdown strategy. Based on those results, we transposed the study in vivo treating mice with CD98 siRNA loaded NPs simultaneously with high fat diet inducing NAFLD.

CD98 siRNA-loaded NPs were significantly uptaken by liver cells, where they attenuated the disease markers of high fat diet-fed mice

Age-matched female C57BL/6 mice were fed a high fat diet for 8 weeks and treated with twice-weekly intravenous injections of CD98 siRNA-loaded NPs (5mg/mL, 100 μ L) or scrambled siRNA-loaded NPs (5mg/mL, 100 μ L). Fluorescent staining of nuclei (DAPI, blue), actin (rhodamine phalloidin, red) and NPs (FITC, green) was assessed (Figure 3A and 3B). Normal patterns (without NPs cytotoxicity observed) were observed for liver samples obtained from mice treated with the scrambled (non-fluorescent) siRNA (Figure 3A), whereas a significant green signal (corresponding to the fluorescent-tagged siRNA) was observed in samples from mice treated with the CD98 siRNA-loaded NPs (Figure 3B). Thus these NPs had significant uptake by liver cells. Next, we examined high fat diet-induced histological changes (i.e., accumulation of lipid vacuoles in the cytosol, fibrosis, etc.) in liver tissues from mice treated with the scrambled siRNA-loaded NPs or CD98 siRNA-loaded NPs. Microscopic analyses of H&E and Sirius red-stained liver sections from these mice revealed the presence of lipid vacuoles (hepatic steatosis) and fibrotic tissue (yellow arrow) in livers from high fat diet-fed mice injected with scrambled siRNA-loaded NPs (Figure 3C and 3D), but not CD98 siRNA-loaded NPs (Figure 3E and 3F). The NAFLD score and fibrosis score were determined using the method developed by Kleiner et al³⁴. The NAFLD activity score was determined to be 7 for the scrambled siRNA-loaded NP liver tissue, which demonstrated high levels of steatosis, lobular inflammation, and a few instances of hepatocyte ballooning (Figure 3G). The fibrosis stage was determined to be 1 for scrambled siRNA loaded NP liver tissue. In contrast, CD98 siRNA-loaded NP liver tissue had a NAFLD score of 0 and no presence of fibrotic tissue. In terms of serum markers, high fat diet-fed mice injected with scrambled siRNA-loaded NPs (similar to control mice) had significantly elevated serum levels of alanine aminotransferase (ALT) (Figure 4A), liver triglycerides, cholesterol, high-density lipoprotein cholesterol (HDLc) and glucose (Figure 4B). In contrast, the corresponding mice treated with CD98 siRNA-loaded NPs had normal

serum ALT and liver triglyceride levels, which represented a 13.7% decrease in triglyceride and 6.7% decrease in HDLc levels compared to that of the scrambled siRNA-loaded NP (Figure 4A and 4B).

Together, these findings indicate that our passive NP-mediated targeting strategy (i.e., due to the ability of liver macrophages to trap particles from the bloodstream) significantly delivered the NPs and released the CD98 siRNA to the liver of mouse. Thus, we next continued examining the beneficial outcome of CD98 siRNA loaded NPs on reducing liver pro-inflammatory response to high fat diet by measuring locally in the liver the expression of inflammation markers.

The protein expression levels of CD98 is downregulated in the livers of mice treated with CD98 siRNA-loaded NPs

Based on our mRNA results, we next assessed the levels of relevant proteins in the liver. Western blot analysis (Figure 4C) showed that the livers of high fat diet-fed mice injected with CD98 siRNA-loaded NPs had dramatically lower CD98 protein expression compared to mice treated with scrambled siRNA-loaded NPs or control mice fed a regular diet. These results indicated that our NP-mediated delivery of CD98 siRNAs successfully downregulates CD98 expression in the liver. The decreased level of CD98 expression has beneficial impacts on liver inflammation in high fat diet-fed mice.

CD98 siRNA loaded NPs IV injections preferentially target the liver locally specifically release siRNA to hepatocytes and Kupffer cells

We explored the biodistribution of FITC tagged NPs on different mice organs; heart, lung, brain, colon, kidney, spleen and liver were collected after 8 weeks of HFD and biweekly intravenous injections of NPs (1mg/mL, 100 μ L). Among all organs collected, only kidney, spleen and liver showed a FITC signal shown in Figure 5. Using the Cellsens dimension fluorescence analysis software, we managed to get fluorescent pictures totally free of tissues autofluorescence signal by optimizing the pictures acquisition of control tissues not treated with FITC-loaded NPs from kidney (Figure 5A), spleen (Figure 5B) and liver (Figure 5C). The fluorescent signal pictures of kidney, spleen and liver showed respectively in Figure 5D, 5E and 5F only show the fluorescent due to FITC loaded NPs. As observed on Figure 5D, kidney had significant uptake of NPs versus a light uptake which was observed for spleen (Figure 5E). Interestingly, mice livers significantly uptake FITC-loaded NPs as shown in Figure 5E, confirming more strongly that the beneficial effect of CD98 loaded NPs on NAFLD was due to direct liver cells uptake.

Complementing those observations, we studied the uptake of FITC loaded NPs during low fat diet. After avoiding tissue auto-fluorescence, as previously mention (Supplementary Figure 3A, 3B and 3C), we noticed that kidney and spleen cells were not uptaking as much NPs as compared with HFD (Supplementary Figure 3D, 3E). Interestingly, liver cells had maintained a relatively high uptake of the FITC loaded NPs also during low fat diet probably due to Kupffer cells activity of phagocytosis (Supplementary Figure 3F).

Finally, we analyzed further the biodistribution at the cellular level within the liver using flow cytometry analysis. Flow cytometry, noted in Figure 6A, 6B, 6C and 6D, showed that

CD98 siRNA loaded NPs mainly target hepatocytes (FITC+ albumin+, Figure 6D) and macrophages like cells (FITC+ CD11b+, Figure 6B), but not dendritic cells (FITC+ CD11c+, Figure 6C). We noticed that liver cells from mice suffering NAFLD were uptaking NPs differently when healthy or receiving HFD. Like cells and hepatocytes from HFD treated mice, had three times more NPs uptake than cells in normal conditions respectively, 1.66 vs 5.32 (Figure 6B) and 6.7 vs 18.0 (Figure 6D). Dendritic cells were not significantly “stimulated” by HFD with very low NPs uptake (below 1 for both conditions, Figure 6C). We also noticed that HFD induced cell death rate in the liver decreased from 63.4 to 50.4 (Figure 6A).

Discussion

CD98 is a type II transmembrane protein that covalently links to one of several L-type amino acid transporters (light chains) to form large, functionally heterodimeric neutral amino acid transport systems^{9,10}. CD98 is constitutively expressed by a variety of tissues, including the liver, which can express different L-type amino acid transporters, including LAT-1 (large neutral amino acid transporter, Na⁺-independent; fetal liver), y⁺-LAT-2 (cationic and large amino acid transporter, Na⁺-independent; liver) and asc-1 (small amino acid transporter, Na⁺-independent; liver)³⁵. In addition to functioning as an amino acid transporter via its extracellular domain^{10,36}, CD98 also regulates cell homeostasis by modulating the activation of integrin^{15,37–40}. Importantly, Yan et al.⁴¹ demonstrated that DSS-induced colitis in mice (a colonic inflammation model) altered the expression of epithelial CD98, which is mediated via interferon-gamma (IFN- γ). The authors further showed that CD98 expression is activated at the transcriptional level in IFN- γ -treated cells, and examined the related mechanisms in the colonic epithelium⁴¹. IFN- γ is present at high levels in pathological liver tissues, including those from NAFLD patients^{42–45}. Similar to IFN- γ , the synthesis of cytokines, such as TNF- α and IL-6, both involved in inflammatory and metabolic alterations, characterizes the earliest phases of different liver injury, leading to the synthesis of other cytokines that, jointly, induce cell migration and initiate healing processes, including fibrosis⁴⁶. A correlation has been found between TNF- α levels and fibrosis degree in NASH patients⁴⁷, as gene expression of either TNF- α or its receptor is significantly elevated in their hepatic and adipose tissues⁴⁸. Similar correlation has been found in NAFLD patients, whose circulating TNF- α were significantly elevated concomitantly with the increase in the activity score, NAS, the histologic scoring system recognized as standard reference in the evaluation and gradation of hepatic inflammation and damage⁴⁹. Also, progression of NAFLD correlates with polymorphisms in the TNF- α promoter region and serum level of soluble TNF receptor 2⁵⁰. A previous study showed that antibody-based inhibition of TNF- α ameliorated the chronic stage of colitis (16). However, systemic antibody treatment is often associated with important side effects^{51,52}. Here, we show that targeted downregulation of CD98, specifically in the liver, can be achieved using siRNA-loaded NPs. In such inflammatory context as described above, local damages (caused by overexpression of IFN- γ , TNF- α and IL-6) on the epithelium of veins and arteries lead to a leakage^{53–56}. NPs potentially used those defects to enter the space of Disse and interact directly with hepatocytes. Consequently, CD98 siRNA-loaded NPs were taken in by both macrophages-like cells and hepatocytes to effectively downregulate CD98

expression at the mRNA and protein levels. This treatment dramatically decreased the progression and symptoms in a mouse model of NAFLD. The inflammation due to the accumulation of lipids in liver cells (inherent to the high fat diet) was significantly decreased, as were the expression levels of all major inflammatory markers, including IFN- γ , which is a direct modulator of CD98⁴¹.

In conclusion, we have shown that CD98 is more than a marker for liver injury; rather, it should be considered a potential therapeutic target for NAFLD. In the future, we hope to improve the utility of our CD98 siRNA-loaded NPs, in particular, by modifying the polymer matrix into a stable bilayer liposome. This modification will allow us to anchor specific ligands on the liposome surface, thereby further increasing the ability of these NPs to target liver cells, and perhaps even a specific cell type within the liver (i.e., hepatocytes, stellate cells, Kupffer cells, etc.).

Supplementary Material

Refer to Web version on PubMed Central for supplementary material.

Acknowledgments

National Institutes of Health of Diabetes and Digestive and Kidney Diseases by the grants K01-DK-097192 (to H.L.).

Grant support: This work was supported by the Chemistry Department and the Center for Diagnostics and Therapeutics of Georgia State University as well as the National Institutes of Health of Diabetes and Digestive and Kidney Diseases through the grant K01-DK-097192 (to H.L.).

References

1. Peverill W, Powell LW, Skoien R. Evolving Concepts in the Pathogenesis of NASH: Beyond Steatosis and Inflammation. *Int J Mol Sci* 2014;15:8591–638. [PubMed: 24830559]
2. Singh S, Allen AM, Wang Z, Prokop LJ, Murad MH, Loomba R. Fibrosis Progression in Nonalcoholic Fatty Liver vs Nonalcoholic Steatohepatitis: A Systematic Review and Meta-analysis of Paired-Biopsy Studies. *Clinical gastroenterology and hepatology : the official clinical practice journal of the American Gastroenterological Association* 2015;13:643–54 e9. [PubMed: 24768810]
3. Gori M, Arciello M, Balsano C. MicroRNAs in nonalcoholic fatty liver disease: novel biomarkers and prognostic tools during the transition from steatosis to hepatocarcinoma. *BioMed research international* 2014;2014:741465. [PubMed: 24745023]
4. Bechmann LP, Hannivoort RA, Gerken G, Hotamisligil GS, Trauner M, Canbay A. The interaction of hepatic lipid and glucose metabolism in liver diseases. *Journal of hepatology* 2012;56:952–64. [PubMed: 22173168]
5. Giorgio V, Prono F, Graziano F, Nobili V. Pediatric non alcoholic fatty liver disease: old and new concepts on development, progression, metabolic insight and potential treatment targets. *BMC pediatrics* 2013;13:40. [PubMed: 23530957]
6. Lomonaco R, Sunny NE, Bril F, Cusi K. Nonalcoholic fatty liver disease: current issues and novel treatment approaches. *Drugs* 2013;73:1–14. [PubMed: 23329465]
7. Lewis JR, Mohanty SR. Nonalcoholic fatty liver disease: a review and update. *Digestive diseases and sciences* 2010;55:560–78. [PubMed: 20101463]
8. Zambo V, Simon-Szabo L, Szelenyi P, Kereszturi E, Banhegyi G, Csala M. Lipotoxicity in the liver. *World journal of hepatology* 2013;5:550–7. [PubMed: 24179614]
9. Yan Y, Vasudevan S, Nguyen HT, Merlin D. Intestinal epithelial CD98: an oligomeric and multifunctional protein. *Biochimica et biophysica acta* 2008;1780:1087–92. [PubMed: 18625289]

10. Deves R, Boyd CA. Surface antigen CD98(4F2): not a single membrane protein, but a family of proteins with multiple functions. *The Journal of membrane biology* 2000;173:165–77. [PubMed: 10667913]
11. Kudo Y, Boyd CAR, Millo J, Sargent IL, Redman CWG. Manipulation of CD98 expression affects both trophoblast cell fusion and amino acid transport activity during syncytialization of human placental BeWo cells. *J Physiol-London* 2003;550:3–9. [PubMed: 12740424]
12. Hara K, Kudoh H, Enomoto T, Hashimoto Y, Masuko T. Enhanced tumorigenicity caused by truncation of the extracellular domain of GP125/CD98 heavy chain. *Oncogene* 2000;19:6209–15. [PubMed: 11175335]
13. Laroui H, Geem D, Xiao B, et al. Targeting intestinal inflammation with CD98 siRNA/PEI-loaded nanoparticles. *Molecular therapy : the journal of the American Society of Gene Therapy* 2014;22:69–80. [PubMed: 24025751]
14. Xue FM, Zhang HP, Hao HJ, et al. CD98 positive eosinophils contribute to T helper 1 pattern inflammation. *PloS one* 2012;7:e51830. [PubMed: 23272174]
15. Nguyen HT, Dalmasso G, Torkvist L, et al. CD98 expression modulates intestinal homeostasis, inflammation, and colitis-associated cancer in mice. *The Journal of clinical investigation* 2011;121:1733–47. [PubMed: 21490400]
16. Kucharzik T, Luger A, Yan Y, et al. Activation of epithelial CD98 glycoprotein perpetuates colonic inflammation. *Laboratory investigation; a journal of technical methods and pathology* 2005;85:932–41. [PubMed: 15880135]
17. Guo X, Li H, Fei F, et al. Genetic variations in SLC3A2/CD98 gene as prognosis predictors in non-small cell lung cancer. *Molecular carcinogenesis* 2014.
18. Kaira K, Oriuchi N, Imai H, et al. CD98 expression is associated with poor prognosis in resected non-small-cell lung cancer with lymph node metastases. *Annals of surgical oncology* 2009;16:3473–81. [PubMed: 19777189]
19. Campbell WA, Sah DE, Medina MM, Albina JE, Coleman WB, Thompson NL. TA1/LAT-1/CD98 light chain and system L activity, but not 4F2/CD98 heavy chain, respond to arginine availability in rat hepatic cells. Loss Of response in tumor cells. *J Biol Chem* 2000;275:5347–54. [PubMed: 10681508]
20. Laroui H, Dalmasso G, Nguyen HT, Yan Y, Sitaraman SV, Merlin D. Drug-loaded nanoparticles targeted to the colon with polysaccharide hydrogel reduce colitis in a mouse model. *Gastroenterology* 2010;138:843–53 e1–2. [PubMed: 19909746]
21. Laroui H, Dalmasso G, Nguyen HTT, Yan YT, Sitaraman SV, Merlin D. Drug-Loaded Nanoparticles Targeted to the Colon With Polysaccharide Hydrogel Reduce Colitis in a Mouse Model. *Gastroenterology* 2010;138:843–U77. [PubMed: 19909746]
22. Laroui H, Geem D, Xiao B, et al. Targeting Intestinal Inflammation With CD98 siRNA/PEI-loaded Nanoparticles. *Molecular Therapy* 2014;22:69–80. [PubMed: 24025751]
23. Laroui H, Grossin L, Leonard M, et al. Hyaluronate-covered nanoparticles for the therapeutic targeting of cartilage. *Biomacromolecules* 2007;8:3879–85. [PubMed: 18039001]
24. Laroui H, Theiss AL, Yan YT, et al. Functional TNF alpha gene silencing mediated by polyethyleneimine/TNF alpha siRNA nanocomplexes in inflamed colon. *Biomaterials* 2011;32:1218–28. [PubMed: 20970849]
25. Laroui H, Viennois E, Xiao B, et al. Fab'-bearing siRNA TNF alpha-loaded nanoparticles targeted to colonic macrophages offer an effective therapy for experimental colitis. *Journal of Controlled Release* 2014;186:41–53. [PubMed: 24810114]
26. Laroui H, Xiao B, Rakhya P, et al. Designing Targeted F4/80-Coated TNFA SiRNA-Loaded Nanoparticles: A Novel Therapeutic Approach to Treat IBD. *Gastroenterology* 2012;142:S341–S.
27. Laroui H, Yan YT, Hang TTN, et al. Silencing of CD98 Expression Using a Nanoparticle-Based Delivery System Ameliorates Induced Colitis in Mice. *Gastroenterology* 2011;140:S10–S1.
28. Frohlich E The role of surface charge in cellular uptake and cytotoxicity of medical nanoparticles. *International journal of nanomedicine* 2012;7:5577–91. [PubMed: 23144561]
29. Laroui H, Viennois E, Xiao B, et al. Fab'-bearing siRNA TNFalpha-loaded nanoparticles targeted to colonic macrophages offer an effective therapy for experimental colitis. *Journal of controlled release : official journal of the Controlled Release Society* 2014;186:41–53. [PubMed: 24810114]

30. Ghaleb AM, Laroui H, Merlin D, Yang VW. Genetic deletion of Klf4 in the mouse intestinal epithelium ameliorates dextran sodium sulfate-induced colitis by modulating the NF-kappaB pathway inflammatory response. *Inflamm Bowel Dis* 2014;20:811–20. [PubMed: 24681655]
31. Xiao B, Laroui H, Viennois E, et al. Nanoparticles with surface antibody against CD98 and carrying CD98 small interfering RNA reduce colitis in mice. *Gastroenterology* 2014;146:1289–300 e1–19. [PubMed: 24503126]
32. Laroui H, Theiss AL, Yan Y, et al. Functional TNFalpha gene silencing mediated by polyethyleneimine/TNFalpha siRNA nanocomplexes in inflamed colon. *Biomaterials* 2011;32:1218–28. [PubMed: 20970849]
33. Theiss AL, Laroui H, Obertone TS, et al. Nanoparticle-based therapeutic delivery of prohibitin to the colonic epithelial cells ameliorates acute murine colitis. *Inflamm Bowel Dis* 2011;17:1163–76. [PubMed: 20872832]
34. Kleiner DE, Brunt EM, Van Natta M, et al. Design and validation of a histological scoring system for nonalcoholic fatty liver disease. *Hepatology* 2005;41:1313–21. [PubMed: 15915461]
35. Nguyen HT, Merlin D. Homeostatic and innate immune responses: role of the transmembrane glycoprotein CD98. *Cellular and molecular life sciences : CMLS* 2012;69:3015–26. [PubMed: 22460579]
36. Boyd CA, Deves R, Laynes R, Kudo Y, Sebastio G. Cationic amino acid transport through system y+L in erythrocytes of patients with lysinuric protein intolerance. *Pflugers Archiv : European journal of physiology* 2000;439:513–6. [PubMed: 10764208]
37. Fenczik CA, Sethi T, Ramos JW, Hughes PE, Ginsberg MH. Complementation of dominant suppression implicates CD98 in integrin activation. *Nature* 1997;390:81–5. [PubMed: 9363894]
38. Hynes RO. Integrins: versatility, modulation, and signaling in cell adhesion. *Cell* 1992;69:11–25. [PubMed: 1555235]
39. Albelda SM. Role of integrins and other cell adhesion molecules in tumor progression and metastasis. *Laboratory investigation; a journal of technical methods and pathology* 1993;68:4–17. [PubMed: 8423675]
40. Zent R, Fenczik CA, Calderwood DA, Liu S, Dellos M, Ginsberg MH. Class- and splice variant-specific association of CD98 with integrin beta cytoplasmic domains. *J Biol Chem* 2000;275:5059–64. [PubMed: 10671548]
41. Yan Y, Dalmasso G, Sitaraman S, Merlin D. Characterization of the human intestinal CD98 promoter and its regulation by interferon-gamma. *American journal of physiology Gastrointestinal and liver physiology* 2007;292:G535–45. [PubMed: 17023546]
42. Zigmond E, Tayer-Shifman O, Lalazar G, et al. beta-glycosphingolipids ameliorated non-alcoholic steatohepatitis in the Psammomys obesus model. *Journal of inflammation research* 2014;7:151–8. [PubMed: 25336983]
43. Baranova A, Schlauch K, Elariny H, et al. Gene expression patterns in hepatic tissue and visceral adipose tissue of patients with non-alcoholic fatty liver disease. *Obesity surgery* 2007;17:1111–8. [PubMed: 17953248]
44. Deng ZB, Liu Y, Liu C, et al. Immature myeloid cells induced by a high-fat diet contribute to liver inflammation. *Hepatology* 2009;50:1412–20. [PubMed: 19708080]
45. Huang W, Metlakunta A, Dedousis N, et al. Depletion of liver Kupffer cells prevents the development of diet-induced hepatic steatosis and insulin resistance. *Diabetes* 2010;59:347–57. [PubMed: 19934001]
46. Tilg H, Diehl AM. Cytokines in alcoholic and nonalcoholic steatohepatitis. *The New England journal of medicine* 2000;343:1467–76. [PubMed: 11078773]
47. Jarrar MH, Baranova A, Collantes R, et al. Adipokines and cytokines in nonalcoholic fatty liver disease. *Alimentary pharmacology & therapeutics* 2008;27:412–21. [PubMed: 18081738]
48. Crespo J, Cayon A, Fernandez-Gil P, et al. Gene expression of tumor necrosis factor alpha and TNF-receptors, p55 and p75, in nonalcoholic steatohepatitis patients. *Hepatology* 2001;34:1158–63. [PubMed: 11732005]
49. Haukeland JW, Damas JK, Konopski Z, et al. Systemic inflammation in nonalcoholic fatty liver disease is characterized by elevated levels of CCL2. *J Hepatol* 2006;44:1167–74. [PubMed: 16618517]

50. Tokushige K, Takakura M, Tsuchiya-Matsushita N, Tani ai M, Hashimoto E, Shiratori K. Influence of TNF gene polymorphisms in Japanese patients with NASH and simple steatosis. *J Hepatol* 2007;46:1104–10. [PubMed: 17395331]
51. Tse BC, Navid F, Billups CA, O'Donnell T, Hoehn ME. Ocular abnormalities in patients treated with a novel anti-GD2 monoclonal antibody, hu14.18K322A. *Journal of AAPOS : the official publication of the American Association for Pediatric Ophthalmology and Strabismus / American Association for Pediatric Ophthalmology and Strabismus* 2015.
52. Aussy A, Girszyn N, Vandhuick T, et al. [Psoriatic arthritis during rituximab treatment of granulomatosis with polyangiitis: A new paradoxical side effect?]. *La Revue de medecine interne / fondee par la Societe nationale francaise de medecine interne* 2014.
53. Meekins JW, McLaughlin PJ, West DC, McFadyen IR, Johnson PM. Endothelial cell activation by tumour necrosis factor-alpha (TNF-alpha) and the development of pre-eclampsia. *Clin Exp Immunol* 1994;98:110–4. [PubMed: 7523006]
54. Chen X, Andresen BT, Hill M, Zhang J, Booth F, Zhang C. Role of Reactive Oxygen Species in Tumor Necrosis Factor-alpha Induced Endothelial Dysfunction. *Current hypertension reviews* 2008;4:245–55. [PubMed: 20559453]
55. Hooper WC, Phillips DJ, Renshaw MA, Evatt BL, Benson JM. The up-regulation of IL-6 and IL-8 in human endothelial cells by activated protein C. *J Immunol* 1998;161:2567–73. [PubMed: 9725257]
56. Yang MC, Chang CP, Lei HY. Endothelial cells are damaged by autophagic induction before hepatocytes in Con A-induced acute hepatitis. *Int Immunol* 2010;22:661–70. [PubMed: 20547544]

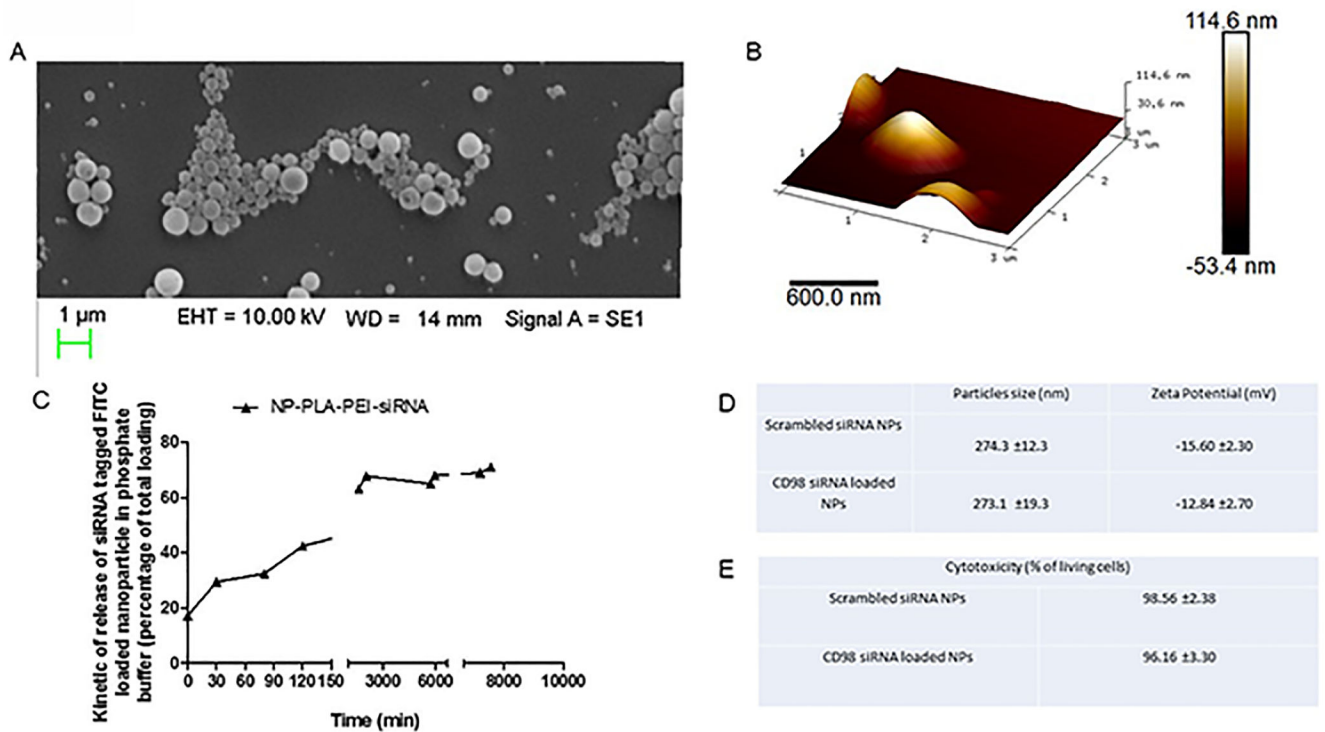


Figure 1: The physicochemical properties of CD98 siRNA-loaded nanoparticles (NPs). (A) Scanning electronic microscopy image of 500 $\mu\text{g}/\text{mL}$ CD98 siRNA-loaded NPs suspension. (B) Atomic force microscopy image of 500 $\mu\text{g}/\text{mL}$ CD98 siRNA-loaded NPs suspension. (C) Kinetic of release of CD98 siRNA complexed with PEI and loaded in NPs (PBS buffer, 37°C) (D) Size distribution and zeta potential (mV) measured by light scattering analysis of CD98 siRNA-loaded NPs and scrambled siRNA-loaded NPs (values represent means \pm SE. Data are representative of n=3 determinations). (E) Cytotoxicity of 1mg/mL CD98 siRNA-loaded NPs and scrambled siRNA-loaded NPs on HepG2 cells for 48h (values represent means \pm SE. Data are representative of n=8 determinations).

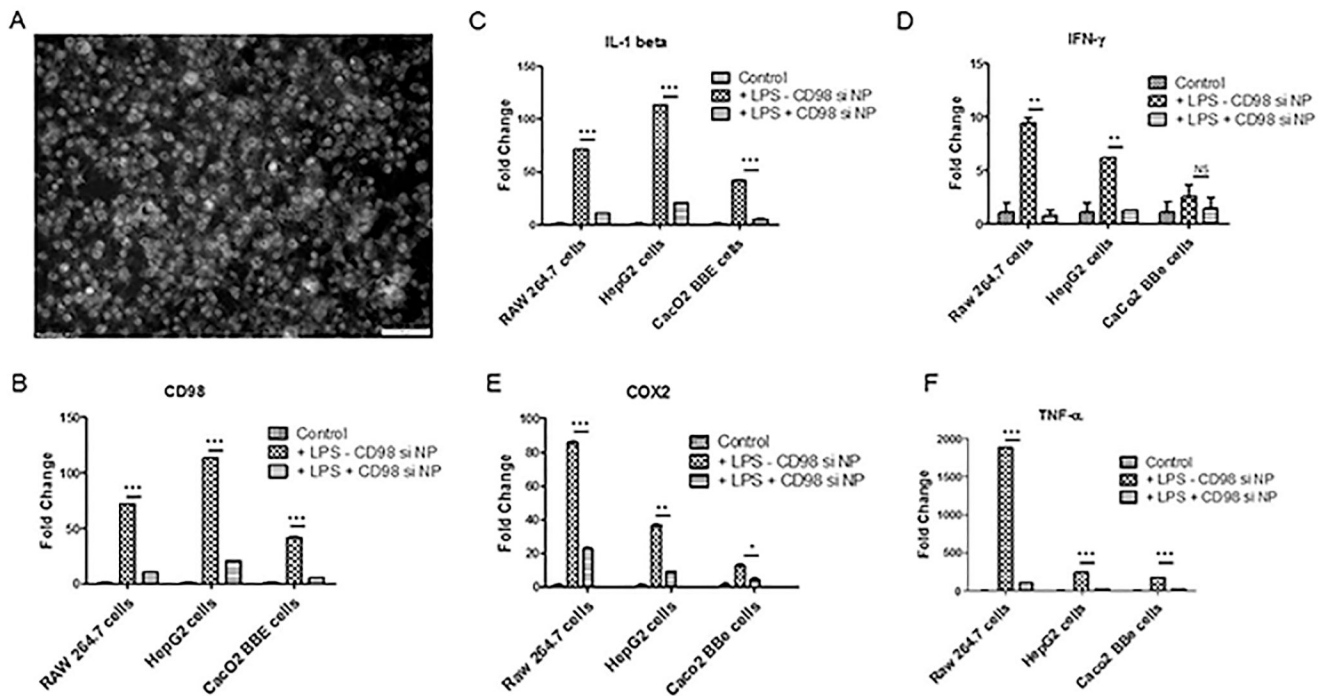


Figure 2: FITC-tagged siRNA/PEI-loaded NPs covered with PLA are rapidly taken up by hepatic cells (HepG2 cells) and the CD98 siRNA is successfully delivered to the cytosol. (A) Fluorescent microscopy of FITC-tagged siRNA/PEI-loaded NPs (200µg/mL, 100µL) uptake by HepG2 cells after overnight contact NPs/ HepG2 cells (gray scale picture). (B) Level of CD98 mRNA expression in non-stimulated HepG2 cells (control) or LPS-stimulated (10 µg/mL LPS for a period of 24h) pretreated overnight with CD98 siRNA-loaded NPs (200µg/mL, 100µL) (+LPS+CD98 si NPs) and scrambled siRNA loaded NPs (200µg/mL, 100µL) (+LPS-CD98 si NPs). (C) Level of IL1-β mRNA expression in non-stimulated HepG2 cells (control) or LPS-stimulated pretreated overnight with CD98 siRNA-loaded NPs (200µg/mL, 100µL) (+LPS+CD98 si NPs) and scrambled siRNA loaded NPs (200µg/mL, 100µL) (+LPS-CD98 si NPs). (D) Level of IFN-γ mRNA expression in non-stimulated HepG2 cells (control) or LPS-stimulated pretreated overnight with CD98 siRNA-loaded NPs (200µg/mL, 100µL) (+LPS+CD98 si NPs) and scrambled siRNA loaded NPs (200µg/mL, 100µL) (+LPS-CD98 si NPs). (E) Level of Cox-2 mRNA expression in non-stimulated HepG2 cells (control) or LPS-stimulated pretreated overnight with CD98 siRNA-loaded NPs (200µg/mL, 100µL) (+LPS+CD98 si NPs) and scrambled siRNA loaded NPs (200µg/mL, 100µL) (+LPS-CD98 si NPs). (F) Level of TNF-α mRNA expression in non-stimulated HepG2 cells (control) or LPS-stimulated pretreated overnight with CD98 siRNA-loaded NPs (200µg/mL, 100µL) (+LPS+CD98 si NPs) and scrambled siRNA loaded NPs (200µg/mL, 100µL) (+LPS-CD98 si NPs). Values represent means ± SE. Data are representative of n=3 determinations. ***P < 0.001, **P < 0.01, *P < 0.05 and NS, not statically significant.

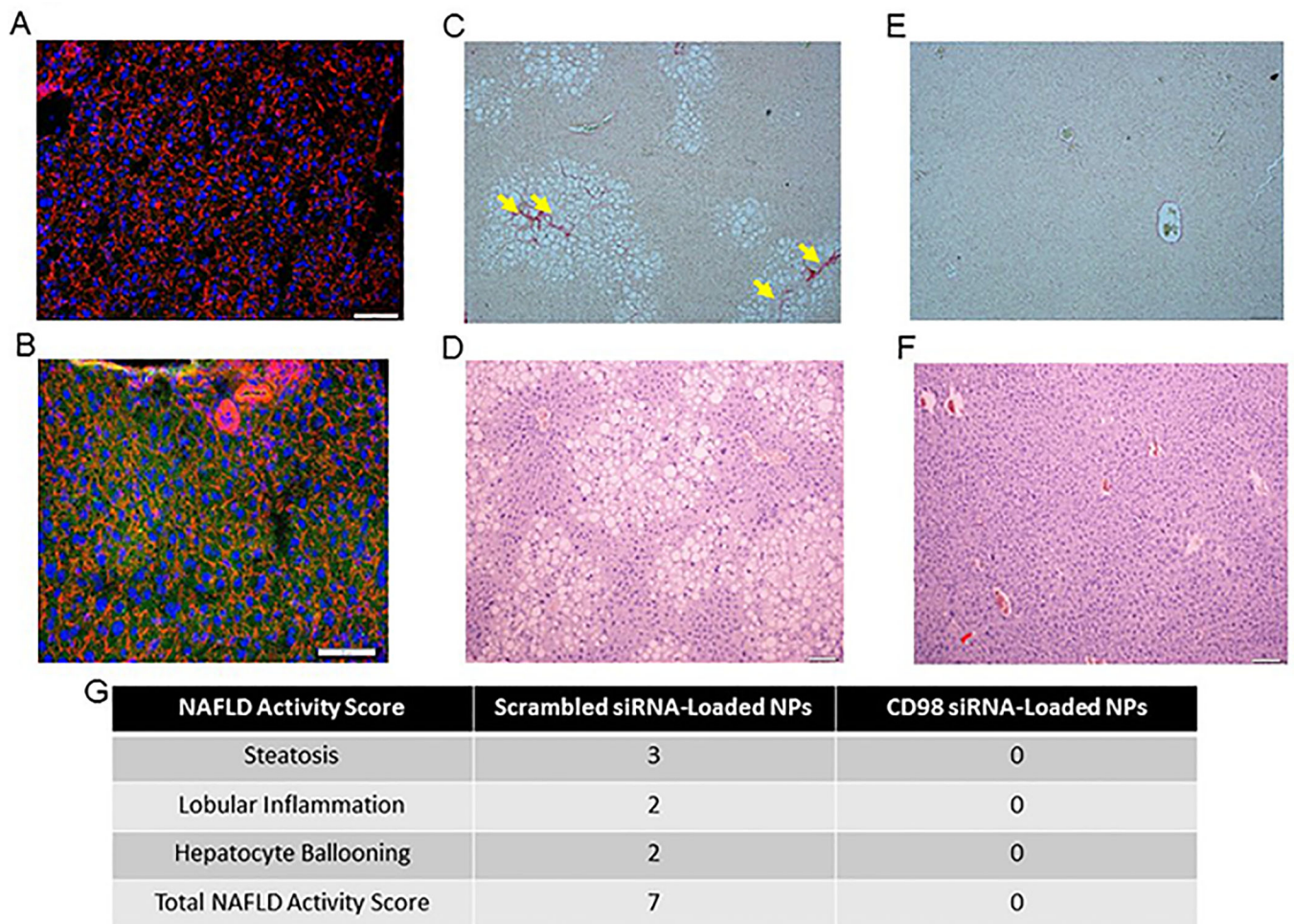


Figure 3: Mice treated with CD98 siRNA-loaded NPs (twice weekly by tail vein injection) show significant liver NP uptake and decreased lipid vacuolization when fed a high fat diet for 8 weeks.

(A, B) Liver pictures of mice injected with scrambled siRNA loaded NPs (5mg/mL, 100 μ L) (A) and FITC tagged siRNA-loaded NPs (5mg/mL, 100 μ L) (B). After intravenous injection of FITC tagged siRNA-loaded NPs (5mg/mL, 100 μ L) (green), mice were sacrificed 4 h later and liver samples were stained for Alexa Fluor 568 phalloidin (red) and DAPI (blue). Representative hematoxylin and eosin (D, F) and Sirius Red (C, E)-stained sections of liver from 8 weeks high fat diet fed mice receiving respectively scrambled siRNA-loaded NPs (5mg/mL, 100 μ L) (C, D) or CD98 siRNA-loaded NPs (5mg/mL, 100 μ L) (E, F) for 12 weeks. Scale bar is 50 μ m. n = 5 mice per group. Hematoxylin and Eosin Y stained liver tissue was scored using the scoring system developed by Kleiner et al³⁴ of mice injected twice weekly with NP treatments (5mg/mL, 100 μ L) (G).

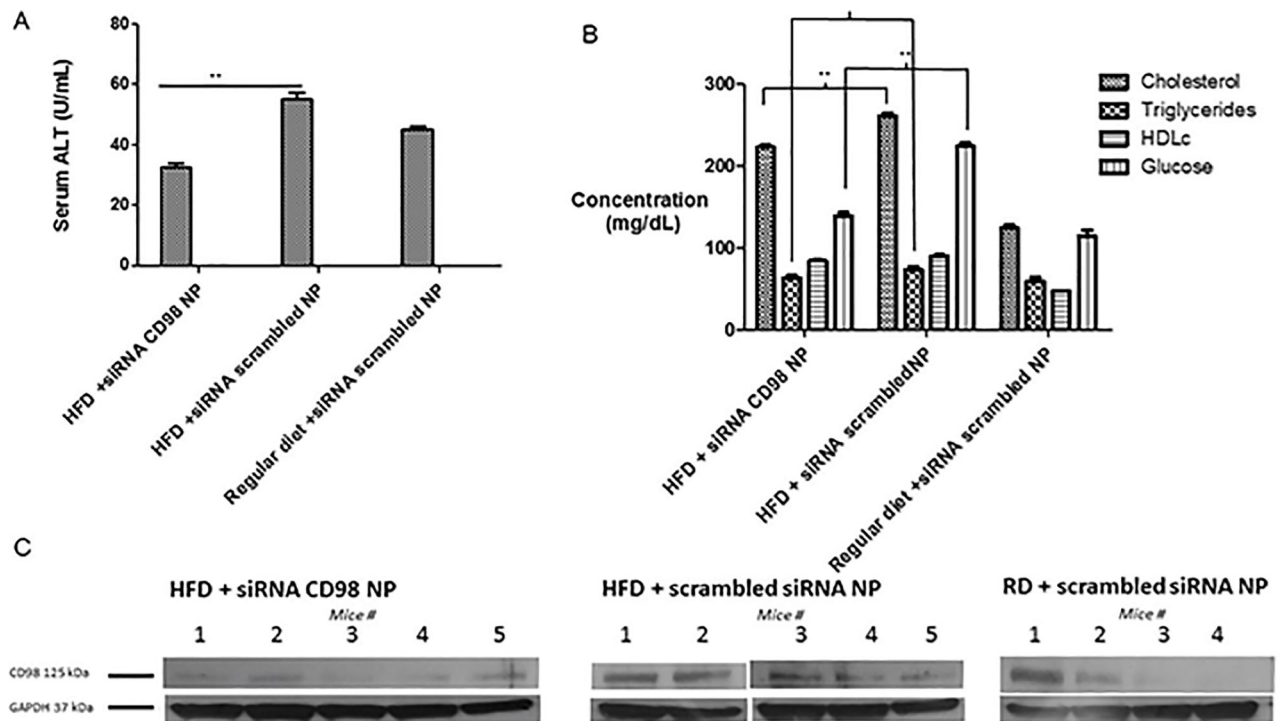


Figure 4: CD98 siRNA-loaded NPs reduce the levels of pro-steatosis markers (blood ALT and lipids) associated with the high fat diet fed mice and suppress CD98 protein expression level of CD98.

(A) Serum ALT levels of mice maintained for 8 weeks on regular diet with injection of scrambled siRNA-loaded NPs (5mg/mL, 100 μ L) (regular diet + scrambled siRNA NP) or high fat diet (8 weeks) with twice a week injections of CD98 siRNA NPs (5mg/mL, 100 μ L) (HFD + siRNA CD98 NP) or scrambled siRNA-loaded NPs (5mg/mL, 100 μ L) (HFD + scrambled siRNA NP). (B) Liver triglyceride, cholesterol, high density lipoprotein cholesterol (HDLc) and glucose levels of mice maintained for 8 weeks on regular diet with injection of scrambled siRNA-loaded NPs (5mg/mL, 100 μ L) (regular diet + scrambled siRNA NP) or high fat diet (8 weeks) with twice a week injections of CD98 siRNA-loaded NPs (5mg/mL, 100 μ L) (HFD + siRNA CD98 NP) or scrambled siRNA-loaded NPs (5mg/mL, 100 μ L) (HFD + scrambled siRNA NP). Values represent means \pm SE. Data are representative of n=5 mice per group. **P < 0.01, *P < 0.05 and NS, not statically significant. (C) Assessment of CD98 in liver from n mice (n being the number of mice used for each group as indicated by the different lines of the WB) fed with regular diet and injected twice a week with scrambled siRNA loaded nanoparticles (5mg/mL, 100 μ L) (regular diet + scrambled siRNA NP) or with high fat diet for 8 weeks and injected twice a week with CD98 siRNA loaded nanoparticles (5mg/mL, 100 μ L) (HFD + siRNA CD98 NP) or scrambled siRNA loaded NP (5mg/mL, 100 μ L) (HFD + scrambled siRNA NP) during 8 weeks. HFD + CD98 siRNA-NPs (n=5), HFD + scrambled siRNA-NPs (n=5), and RD + scrambled siRNA-NPs (n=4). n represent the number of mice for each group.

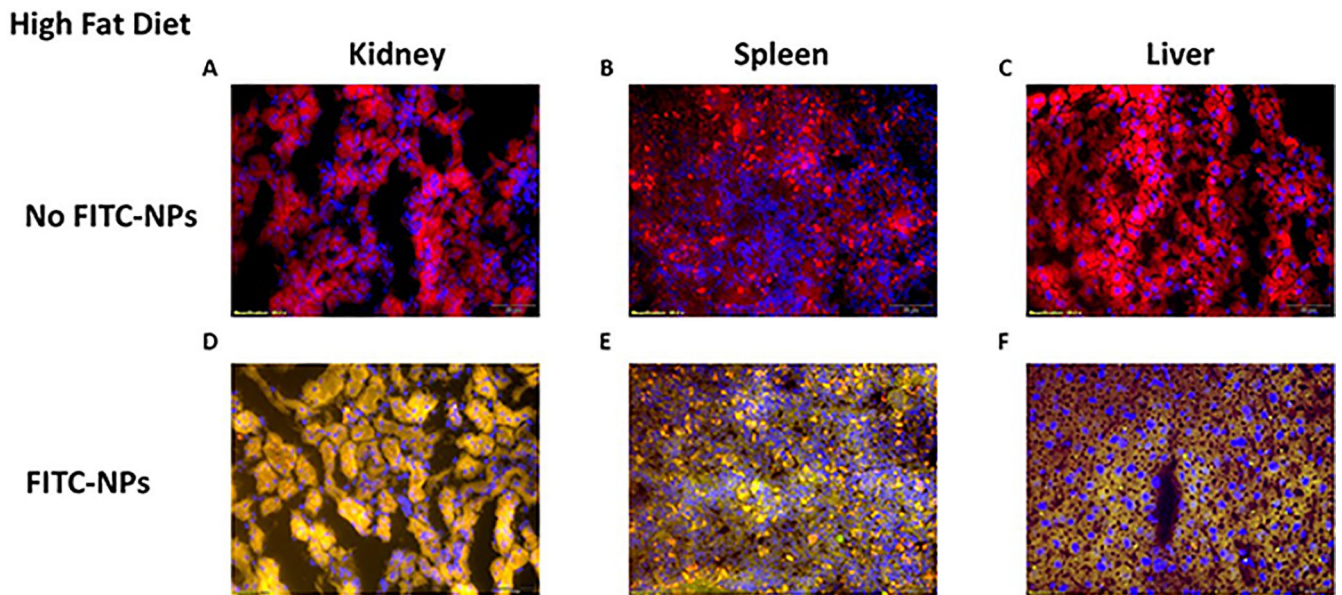


Figure 5: Biodistribution study relative to liver, kidney, and spleen demonstrated significant uptake of the siRNA FITC-loaded NP while mice received HFD.

Histology after tail veins intravenous injections of FITC tagged siRNA-loaded NPs (5mg/mL, 100 μ L) (green), mice were sacrificed and (A, D) kidney, (B, E) spleen, and (C, F) liver samples were stained for Alexa Fluor 568 phalloidin (red) and DAPI (blue). Mice were fed a high fat diet for 8 weeks along with biweekly tail vein intravenous injections of FITC-loaded NPs (5mg/mL, 100 μ L). Scale bar is 50 μ m.

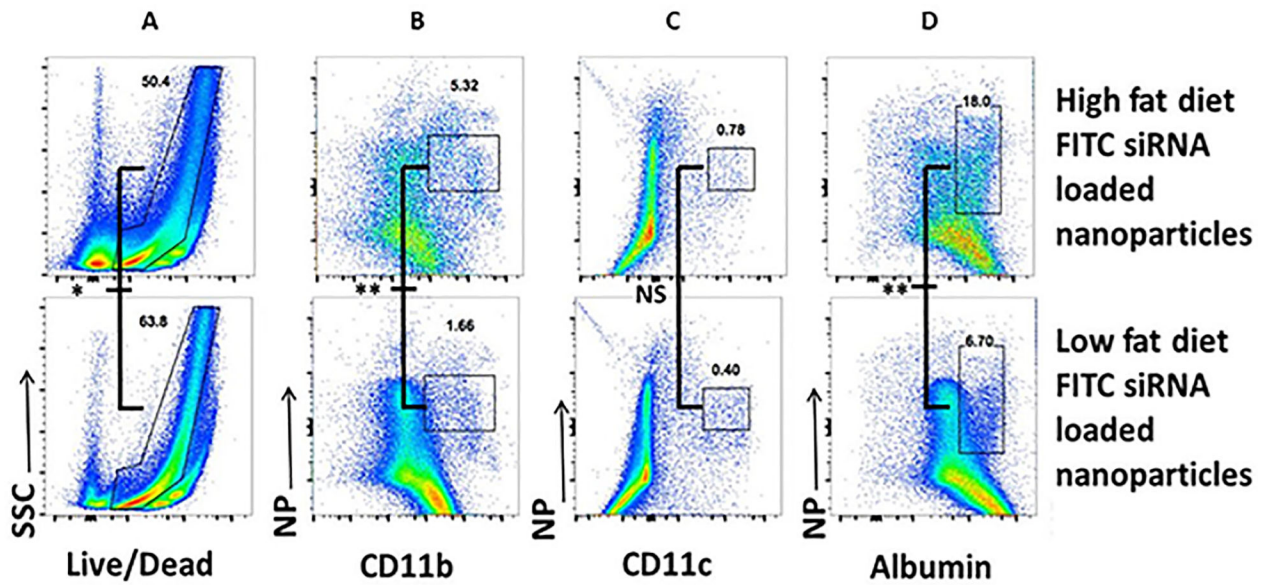


Figure 6: Flow cytometry analysis indicating that biweekly injection of CD98 siRNA-loaded NPs is significantly uptake by hepatocytes and macrophage-like cells compared to dendritic cells. Representative FACS plots illustrating the gating strategy utilized to define live cells (A), macrophages like cells (B), dendritic cells (C) and hepatocytes (D) for mice biweekly injected with FITC-loaded NPs (5mg/mL, 100 μ L) and receiving or not HFD. Cells were gated as followed for hepatocytes CD45-MHC class II-F4/80-CD11b-CD11c-albumin+, macrophages-like cells CD45+MHC class II+F4/80+CD11b+CD11c- cells and dendritic cells CD45+MHC class II+ F4/80-CD11b+CD11c+. Values represent means \pm SE. Data are representative of n=5 mice per group. **P < 0.01, *P < 0.05 and NS, not statically significant.